Journal of Theoretical and Applied Physics (JTAP), Vol.14, No. 4, Pages 399-409 , 2020
Received 15 February 2020 ; Accepted 21 September 2020 ; [http://dx.doi.org/10.1007/s40094-020-00396-z]

Industrial application of apodized gas sensor for on-line and in situ measurement of CO and CO_2 concentration

Seyedali Hosseinzadeh Salati, Alireza Khorsandi*, Saeed Ghavami Sabouri

Abstract
The performance of an apodized gas sensor is demonstrated through simultaneous detection of CO and CO_2 absorption lines around 1.57 μm in the recuperator channel of a gas-fired industrial furnace at Shahid Montazeri power plant (SMPP) industry. This led to the concentration measurement of targeted molecules as less than $\sim$1% and 9.5%, respectively, at atmospheric pressure and 350^{o}C, indicating close consistency with the reference data reported by SMPP. A minimum detectable absorption of $\sim 0.4\times10^{-3}$, corresponding to a detection sensitivity of $\sim 4.8\times10^{-9}$ cm^{-1}Hz$^{-1/2}$ is measured in this application.

Keywords
Wavelength modulation spectroscopy, Apodized gas sensor, Tunable diode laser.

Department of Physics, University of Isfahan, Isfahan, Iran
*__Corresponding author__: a.khorsandi@phys.ui.ac.ir

1. Introduction

Since most of the hazardous and pollutant molecules such as carbon monoxide (CO), nitric oxide (NO), methane (CH_4) and carbon dioxide (CO_2) exhibit sufficient absorption strengths in the near-infrared (NIR) region, much efforts have been conducted toward the development of new and simple spectroscopic methods. Tunable diode laser absorption spectroscopy (TDLAS) has shown very promising tools for in-situ and online process control of industrial emissions, quantification of medical compounds and for security purposes as well [1]. Since the development of high efficient semiconductor lasers in the past 25 years, a remarkable improvement to the gas diagnostic systems has been attained using a numerous TDLAS schemes [2]. Because of high performance and fast response characteristics of NIR-TDLAS base gas sensors, they have reached the expected detection sensitivities down to ppbv levels required, for example, in quantitative monitoring of medical markers in the human exhaled breath [3]. Those sensors have very simple and robust setup and are compatible with many low-loss and cost-effective elements like optical fibers and glass-based lenses and windows. The essential requirements for an ideal gas sensor is a light source possessing high spectral purity and beam quality, long time stability and broad tunability, wide dynamic range and immunity to environmental disturbances. Most of the above requirements have been met by the well-established continuous wave (CW) and room-temperature operated, distributed feedback (DFB) [4] and quantum cascade (QC) [5] lasers. These lasers are receiving a great interest in the NIR due to their excellent properties including single-mode operation, high spectral purity and sufficient optical power which make a DFB laser very competitive to other conventional sources such as Fabry-Perot-based and vertical cavity surface emitting lasers (VCSEL). However, scientific reports on a VCSEL indicate that because the optimum laser gain material and mirror material are incompatible with the epitaxial grown their developments is still a technological challenge [6]. As regards, in a DFB laser the key element is a Bragg grating incorporated in the laser structure which guarantees reaching unique characteristics like narrow linewidth of $\sim$10 MHz, single mode operation and compact size. Moreover, by any III/V-based materials being used in the fabrication of a DFB laser, broad wavelength range of 760 nm up to $\sim$ 3 μm is possibly achieved [7]. Accordingly, several approaches have been represented to attain new demonstrations for a DFB laser. Recently, Liu et al. [8] has introduced an organic DFB laser as an excitation source in Raman spectroscopy. They employed a high quality resonator along with a novel encapsulation method to improve the laser output efficiency to $\sim$7.6% and provide the laser linewidth of $\sim$83 MHz. In 2013 very low threshold apodized distributed feedback fiber laser (DFB-FL) is theoretically analyzed and experimentally fabricated by Qi et al. [9] to obtain laser output power of $\sim$18 μW at $\sim$100 mW of pump power in a backward pumping scheme. The linewidth of such DFB-FL light source was measured 20 kHz at 60 mW of input pump. Owing to the many advantages of using inexpensive and large capacity optical fibers, numerous reports on the fiber-based DFB spectrometers have been conducted to introduce very flexible and in situ gas sensors. One example is reported by Bagheri et al. [10] after which a fiber-coupled DFB laser operating near $\sim$2 μm wavelength was

fabricated for high power LIDAR transmitters for mapping the CO_2 concentration in the atmosphere. It was capable of delivering more than 35 mW within a less than 200 kHz of intrinsic linewidth. Furthermore, by a fiber-pigtailed configuration the spectrometer becomes less sensitive in alignment, making the sensor specific for applications in combustive industries and harsh environments. This is particularly advantageous for fabricating multi-objective fiber sensors based on multiplexing technique using DFB lasers emitting around 1.5 μm which enables very wide measurement bandwidth. Subsequently, many fiber-coupled DFB lasers operating in 1.57 μm band has been extensively studied and developed for fabricating various types of laser sensors [11, 12]. On the other hand, a combination of inexpensive 1.57 μm NIR lasers and detectors with optical fibers utilizing as a sensor element provides minimum loss and dispersion. An experimental demonstration is represented by Yu et al. [13] in which a multiplexed DFB laser sensor is developed for non-intrusively measure of C_2H_2 concentration with a minimum detectable absorbance of 2.1×10^{-4}. The weakness of overtone transition lines in this band can be compensated to a large extent by a proper choice of particular spectroscopic technique. One solution is to increase the absorption path length over tens of kilometers using a high finesse cavity filled by the gas sample. Hereupon, cavity ringdown spectroscopy (CRDS) has been implemented to attain very sensitive detection based on the measurement of the decay rate of light intensity travelling between two ultra low-loss dielectric mirrors of the cavity. A new type of CW-CRDS is designed by Li et al. [14] in 2013 based on the control of ringdown time to obtain a SNR improved by three orders of magnitude for absorption coefficient measurement of C_2H_2 near 1530.9 nm. The main disadvantage with this technique is that CDRS technique requires very high quality and low loss cavity mirrors which make the setup costly. An alternative and effective option is to use a combination of conventional absorption cells with the modulation of the laser source [15]. Hence, wavelength modulation spectroscopy (WMS) is introduced as a well-established approach which is based on the effective reduction of detection noise mostly caused by 1/f noise. This technique is established by the modulation of the operating wavelength of a DFB laser up to several kHz to a few MHz. In the most cases, the modulated signal is detected at twice the modulation frequency by using a lock-in amplifier set to 2f. The application of the WMS-2f technique is widely investigated and reported by numerous research groups used, for example, for tracing very low concentrations in routine clinical care up to ppt level [16, 17]. A case example is the sulfur dioxide detection based on quartz-enhanced photoacoustic technique along with a WMS-2f method to obtain a minimum detection limit of 63 ppbv [18]. However, the major challenge to the final results is the distinguishing of the absorption features from the baseline variations owing to the intensity modulation of the laser beam. This has led to the generation of a nonzero background for 2f signal. It is known as residual amplitude modulation (RAM) that needs particular care in the determination of absolute absorbance. In harsh and high-pressure combustion where a non-absorbing baseline is not attainable, 1f signal can be used as a baseline to normalize any change in the intensity of the incident laser beam and in undesirable electronic and optical perturbations. It is simply accomplished by dividing the WMS-2f signal by WMS-1f signal. This has led to the generation of a calibration-free WMS-2f/1f signal which is free from misalignments and insertion noises. The first experimental demonstration of such calibration-free WMS-2f/1f is reported by Li et al. [19] and developed by Reiker et al [20] in 2009 for temperature and concentration measurement of H_2O and CO molecules between 1.3 and 2 μm within a scramjet combustor. The same technique has recently been exploited by Goldenstein et al. [21] to measure the H_2O concentration near 1.4 μm in a high-pressure and temperature combustion. Despite the benefits of using the WMS-2f/1f technique, it is faced by several drawbacks which limits the use of this method. Those include beyond the optical thin limit the WMS-2f/1f signal tends to infinity in the wings and the absorption trace displaces from the line center. This causes an uncertainty and unavoidable systematic error to occur in the measurement. In order to overcome the explained difficulties a new approach has recently been introduced in our previous work [22] based on the apodizing of the WMS-1f signal to extend the application of the WMS-2f/1f method regardless of optical limits. We found very good agreement between the theory and experiment through trace detection of R(9) CO absorption overtone line at atmospheric pressure around 2.33 μm.

In the present work the performances of the apodized calibration free WMS-2f/1f technique is shown through quantitative measurement of CO and CO_2 concentrations in the recuperator channel of the gas-fired 1600 MW Shahid Montazeri power plant (SMPP) located in the Isfahan suburb. The apodized sensor consists of a fiber-coupled NIR-DFB laser operating at 1.57 μm and a multi-pass absorption as head probe that provides an effective path length of $\sim$8 m inside a 2-m-long cylindrical steel tube by means of three embedded reflecting prisms. The field results have been confirmed by a reference investigation accomplished by simulation and experimental measurements of R(1) CO and R(12) and R(14) CO_2 absorption lines inside a 3-m-long single pass pre-vacuumed laboratory cell. The results of this study indicate that the fabricated sensor is capable of on-line, in situ and sensitive detection of such important combustion products which are the challenges of the global climate and environment.

2. Concepts of apodized WMS-2f/1f method in brief

The absorption of a monochromatic laser beam crossing a gas sample is described by Beer-Lambert law that is

$$I(\nu) = I_0(\nu)\exp[-\alpha_{abs}(\nu)] \quad (1)$$

where $I(\nu)$ and $I_0(\nu)$ are the intensity of transmitted and incident laser beam and α_{abs} is the frequency-dependent ab-

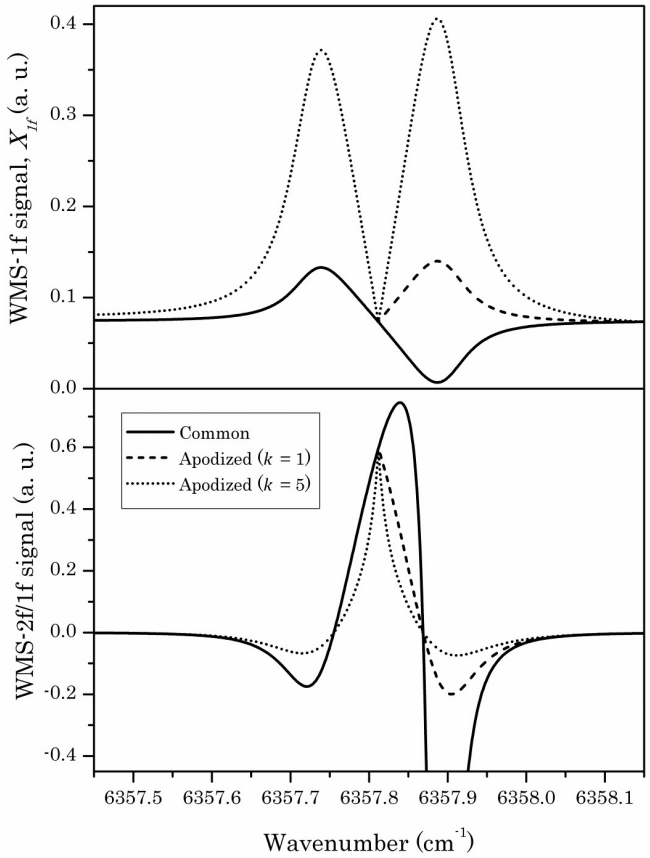

Figure 1. The effect of scaling factor on the WMS signals simulated for R(1) CO absorption line centered at 6357.814 cm^{-1}. The absorbance of CO gas is assumed $\alpha(\nu)$ =0.035 which implies that the gas sample is very close to the optically thick region because the right wing of the X_{1f} signal is approaching zero. Simulation is performed at room temperature and modulation frequency and index are assumed 3 kHz and 2.2, respectively.

sorbance of the sample. The latter is further dependent on the linestrength of transition and partial pressure of the absorber. The establishment of WMS method is based on the application of a sine wave of angular frequency ω to the laser injection current while the laser wavelength is simultaneously scanned over a certain absorption line using a sawtooth voltage ramp, then detection of the modulated absorption at 2ω using a lock-in amplifier. This led to the modulation of sample absorbance as

$$\exp\{-\alpha_{abs}[\bar{\nu}+a\Delta\nu_{1/2}\cos(\omega t)]\}= \sum_{k=0}^{\infty} H_k(a,\Delta\nu_{1/2},\bar{\nu})\cos(k\omega t) \quad (2)$$

where $\bar{\nu}$ is the average laser frequency during a modulation period, $\Delta\nu_{1/2}$ is the HWHM of absorption line and a is the modulation index. Here $H_k(a,\Delta\nu_{1/2},\bar{\nu})$ are symmetrical and anti-symmetrical components of the Fourier expansion. At

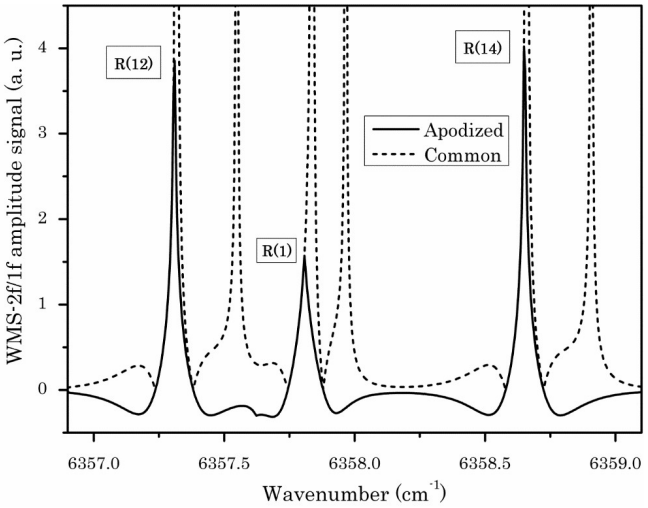

Figure 2. The simulation results of common and apodized WMS-2f/1f techniques for R(1) CO and R(12) and R(14) CO_2 absorption lines centered at 6357.814 cm^{-1}, 6357.312 cm^{-1} and 6358.654 cm^{-1}, respectively. To provide the required comparison scaling k factor is set to one. Modulation frequency and index are assumed 3 kHz and 1.5, respectively, for 1 mA of modulation current.

the same time the laser intensity is inevitably modulated according to

$$I_0(t)=\bar{I}_0[\sum_{m=1}^{\infty} i_m\cos(m\omega t+\psi_m-m\psi)] \quad (3)$$

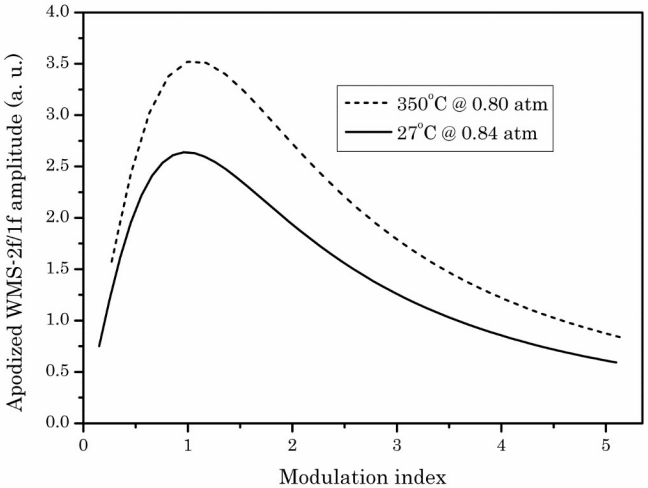

Figure 3. Variation of apodized WMS-2f/1f amplitude with modulation index provided using practical values associated with R(12) CO_2 absorption line which is simulated under different temperature and pressure conditions for 8-m-long absorption path length and 10% CO_2 gas in the atmospheric air. In the simulation modulation index and k factor has been set for 3 kHz and one, respectively.

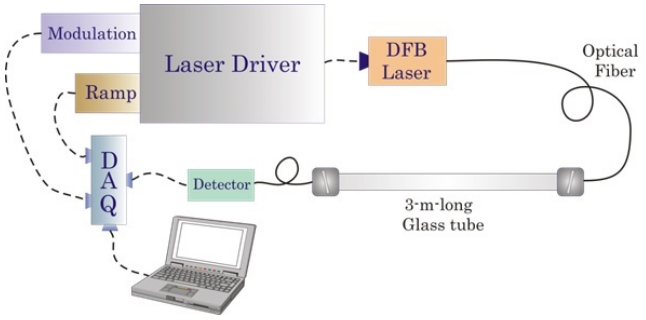

Figure 4. Experimental apparatus arranged in the laboratory to evaluate the potential of using the Calibration-free apodized WMS-2f/1f gas sensor in the field application at SMPP. It employs an NIR-DFB laser and a 3-m-long single pass absorption cell for simultaneous CO and CO_2 detection to provide a reference measurement. To avoid the interference effects the side windows of the glass tube are slightly inclined.

where $\bar{I}_0$ is the average intensity over a modulation period, i_m is the mth modulation coefficient, ψ_m is the initial phase shift between mth harmonics of modulated intensity and reference frequency and ψ is the initial arbitrary phase of modulation. Scanning of the target absorber will be performed through a ramp voltage imposed on the input current such that

$$\bar{I}_0 = I_{max}(1 - \frac{t}{T}) + I_{min}(\frac{t}{T}) \quad (4)$$

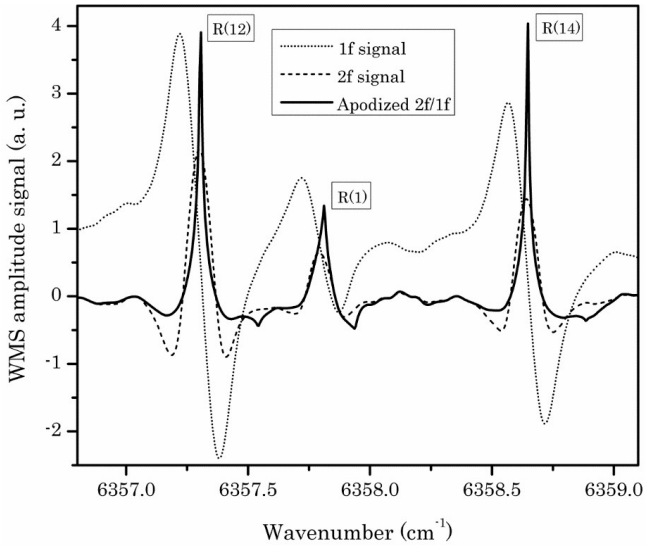

Figure 5. Experimental trace of apodized WMS-2f/1f signal of R(1) CO and R(12) and R(14) CO_2 absorption lines centered at 6357.814 cm^{-1}, 6357.312 cm^{-1} and 6358.654 cm^{-1}, respectively, inside a 3-m-long single pass glass tube kept at ~690±0.1 mbar of total pressure containing 68% CO and 32% CO_2 gases. Modulation frequency and index are set at 3 kHz and 1.5, respectively. The scaling factor k is fixed at 1.5.

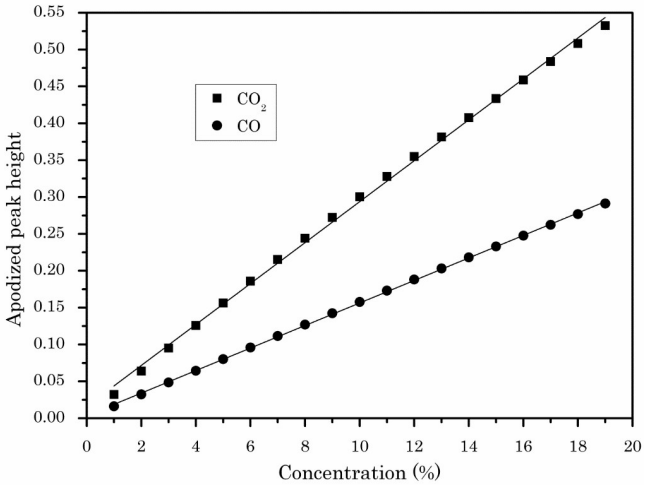

Figure 6. The variation of apodized WMS-2f/1f peak heights versus CO and CO_2 concentrations for being used in the oncoming field measurement for gas percentages determination which will be established at SMPP area.

where T is the ramp period, t is the elapsed time from the starting point of the ramp and I_{max} and I_{min} are respectively the intensities of the DFB laser beam at both ends of the ramp. By substituting Eqs.(2) and (3) into Eq. (1) and assuming that $\bar{I}_0$ is relatively constant during the laser beam is sweeping over a modulation period, the nth harmonic of the modulated signal can be extracted from the detector signal behind a lock-in amplifier that has a sufficient bandwidth. A lock-in amplifier multiplies the detector signal by a desired modulation har-

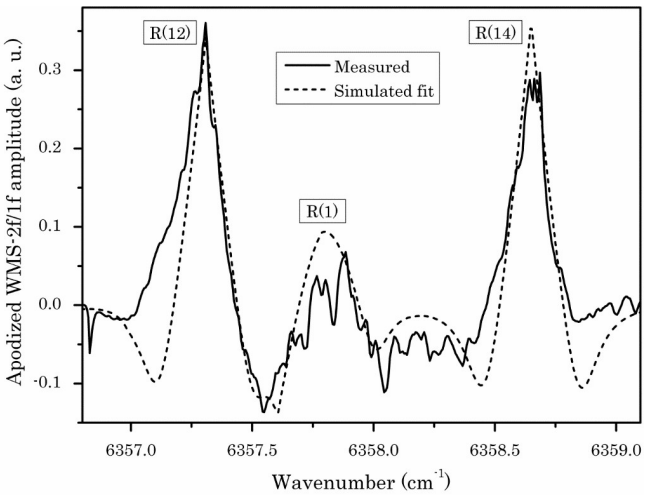

Figure 7. The in situ and sensitive detection of the R(1) CO and R(12) and R(14) CO_2 absorption lines in the smoke released from the burned coal collected in a pre-concentrator and flowed toward the 3-m-long absorption cell with a flow rate of ~0.5 lit/min. The fitted curve is the simulated trace provided to estimate the CO and CO_2 concentrations in the extracted smoke. In either trace the modulation frequency and the scaling k factor are 3 kHz and 3, respectively.

Table 1. Characteristics of the R(12) CO_2 line used in plotting Fig. 3 based on the data reported in Hitran 2019. The data in the first row are calculated according to the SMPP condition.

Selected absorption line	Pressure (atm)	Temperature (^OC)	Doppler linewidth $\Delta\nu_D$cm^{-1}	Lorentzian linewidth $\Delta\nu_L$cm^{-1}	Voigt linewidth $\Delta\nu_V$cm^{-1}
R(12) CO_2	0.84	27	0.007	0.068	0.069
	0.80	350	0.011	0.065	0.067

monic and filters out the others by making use of an internal low-pass filter. Eventually, the nth harmonic at the lock-in output is

$$X_{nf} = \frac{G\bar{I}_0}{2}[H_k + \frac{1}{2}\sum_{m=1}^{\infty} i_m(H_{k+m} + (1+\delta_{km})H_{|k-m|}) \cos(\psi_m - m\psi)] \quad (5)$$

Note that all Y-components can be vanished by setting an arbitrary detection phase equal to zero. Specifically, the first and second harmonic signals are

$$X_{1f} = \frac{G\bar{I}_0}{2}[H_1 + i_1(H_0 + \frac{H_2}{2})\cos(\psi_1 - \psi) + \frac{i_2}{2}(H_1 + H_3)\cos(\psi_2 - 2\psi) + ...]$$

and

$$X_{2f} = \frac{G\bar{I}_0}{2}[H_2 + \frac{i_0}{2}(H_1 + H_3)\cos(\psi_1 - \psi) + i_2(H_0 + \frac{H_4}{2})\cos(\psi_2 - 2\psi) + ...] \quad (6)$$

where G is the electro-optic gain that appears in all X_{nf} components. In normalizing the X_{2f} by X_{1f}, the resultant WMS-2f/1f signal becomes independent of both G and laser intensity variations. Throughout the non-absorbing portions of the signal $H_n = \delta_{n0}$ which implies that the higher harmonics with $n > 0$ are approaching zero. This makes H_0 very significant in X_{1f} expression, providing a non-zero baseline for the normalization of the other X_{nf} components. Due to the lower relative noise and higher intensity, X_{2f} is of great interest for making such normalized signal. Nonetheless, compared to the direct absorption spectroscopy method, WMS-2f/1f technique is very susceptible to the type of utilized gas sample, environmental conditions and to the laser source characteristics such as its slope efficiency and tuning rate. Moreover, it needs periodic calibration, making it inconvenient for fabricating a reliable and long-term operating gas sensor. Above all, as it was experimentally confirmed, by the division of relatively symmetrical X_{2f} signal by anti-symmetrical X_{1f} signal the peak of the common WMS-2f/1f signal deviates from the line center and being much pronounced when the concentration exceeds the optical thin limit. Moreover, it was observed that for optically thick samples the common WMS-2f/1f signal tends to the infinity in the wing. As a result, an uncertainty will be occured in the concentration measurement which drops the performance of the common method for using in many practical applications particularly in the combustive environments. It is worthy to note that the range of optical limit depends not only on the type of molecular gas sample but also on the center frequency of the investigating targeted abosrtpion line. Thus, for example, for the selected CO and CO_2 lines that are being considered in this work the optical thin limit is different. The explained problems above can be amended by the apodized WMS-2f/1f in which the X_{1f} signal is symmetrized by averaging of the 1f signal during a modulation period to obtain

$$X_{1f}^{apodized} = X_{1f}^{baseline} + k|X_{1f} - X_{1f}^{baseline}| \quad (7)$$

where $X_{1f}^{baseline} \approx (G\bar{I}_0/2)i_1\cos(\psi_1 - \psi)$ is obtained by equating $H_0 = 1$ and neglecting all $H_n(n > 0)$ coefficients for non-absorbing portion of the X_{1f} signal. In Eq. (7), k is referred to as arbitrary scaling factor which plays an important role in sharpening and narrowing of the resultant WMS-2f/1f signal. Eventually, we have

$$X_{1f}^{apodized} = G\frac{\bar{I}_0}{2}\{i_1\cos(\psi_1 - \psi) + k|H_1 + i_1(H_0 + \frac{H_2}{2} - 1) \times \cos(\psi_1 - \psi) + \frac{i_2}{2}(H_1 + H_3)\cos(\psi_2 - 2\psi)\} \quad (8)$$

The inequality in Eq. (8) is because of the presence of unavoidable RAM signal due to the modulation of laser intensity. The main idea behind the selection of scaling factor is to obtain a minimum uncertainty and to reduce the X_{1f} signal fluctuations. Fig. 1 highligths the impact of the k factor on the WMS signals simulated for R(1) CO absorption line.
As can be seen, due to reaching the descending branch of X_{1f} very close to zero the common WMS-2f/1f is tended to infinity and the signal peak is also displaced toward longer wavenumbers. This behavior is clearly avoided by application of the apodized method on the data. This is performed through effecting the k factor on the X_{1f} signal where the singularity of 2f/1f division due to the limitation of optically

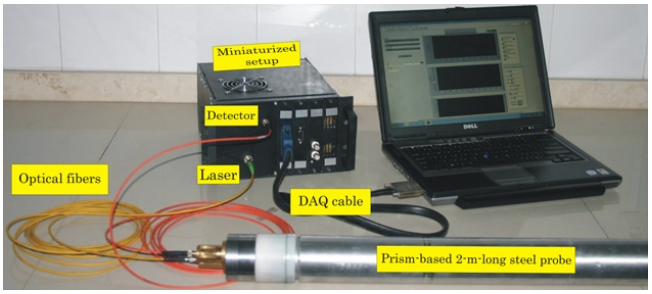

Figure 8. The miniaturized apodized WMS-2f/1f spectrometer for using at SMPP environment. The whole of the device is placed completely in an aluminum box and connected to the sensor head using the two utilized optical fibers (Tramco, 0652D and Thorlabs, M29L05).

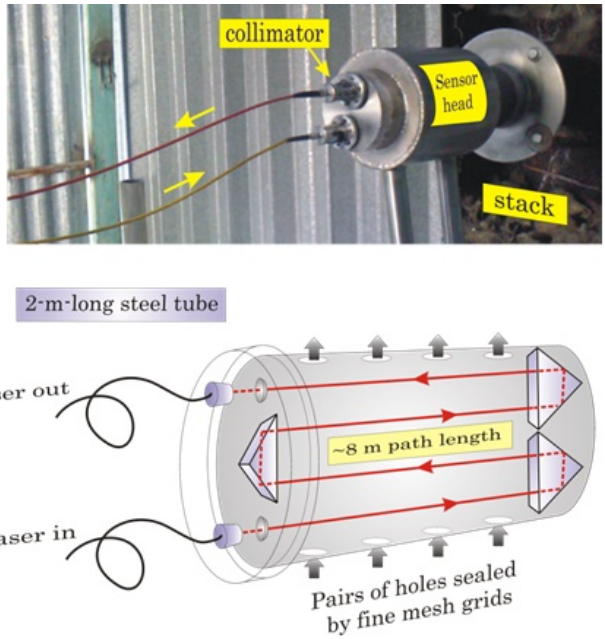

Figure 9. (top) Fabricated probe placed inside the provided stack for exposing the smoke. (bottom) Schemetic of the sensor head containing three reflecting 45^o prisms to provide an effective absorption path length of ∼8 m inside a 2-m-long steel tube. Two fiber-coupled collimators are responsible for the alignment of setup configuration. Vertical arrows indicate the direction of smoke flow inside the probe.

thick sample is occured. Moreover, the greater the k factor is, the sharpness of the aposized WMS-2f/1f is increased without either the displacement of the line center or significant uncetratity due to the infinity tending. As a result, the apodized WMS-2f/1f method is potentially capable of providing a lineshift-free signal and calibration-free measurement without causing uncertainty when using optical thick samples. This is particularly very advantageous in practical applications in the environment containing high concentration molecules and noises which misalign the optical setup and calibration of the sensor is frequenly required. Subsequently, the preference of the apodized WMS-2f/1f approach is simulated and compared with the common WMS-2f/1f method in Fig. 2. The calculation is accomplished beyond the optically thin limit using the practical data associated with R(1) CO and R(12) and R(14) CO_2 absorption lines as those used in the oncoming experimental section of this work. To provide the figure, a mixture of 68% CO_2 and 32% CO gases are assumed in the calculation, corresponding to the absorbances of 0.074, 0.077 for R(12) and R(14) CO_2 line, respectively, and of 0.075 for R(1) CO line.

As it can be seen from the above plot, a relatively large uncertainty is induced to the common WMS-2f/1f due to the peak-to-peak increase occurring in the WMS-1f trace for optically thick samples. This is in contrast with the apodized trace where it is inclined toward a certain value along with enhanced signal resolution in the output and keeping the physical characteristics of the absorption lines. Furthermore, the sharpness of the signal is very advantageous in measuring the line shift in a mixed sample including two or more overlapped absorption lines within the scan range of a DFB laser source. However, as previously illustrated in Fig. 1, it is further demonstrated that the peaks of the common WMS-2f/1f signal are slightly displaced from the line center owing to the normalization of a symmetrical 2f signal by an anti-symmetrical 1f signal. It should be noted that the effects of broadening mechanisms such as Doppler and pressure broadening which are significantly present in harsh environmental areas, will broaden the lines and alters the apodized amplitude. This can be avoided by the variation of modulation index to achieve maximum amplitude and higher signal resolution in the output of the utilized lock-in amplifier.

Consequently, based along the practical values the effects of modulation index on the apodized WMS-2f/1f signal is investigated and simulated in Fig. 3 for R(12) CO_2 absorption line. In order to indicate the significance of the line broadening and its effect on the optimum modulation index, calculation has been performed for different circumstances according to the laboratory condition and the case example of industrial combustion provided by SMPP.

Referred to the simulated results depicted in Fig. 3, Doppler and pressure HWHM linewidths of the selected line are listed in Table.1.

Apparently, it can be understood from Fig. 3 that the maximum amplitude of the apodized WMS-2f/1f signal is obtained at modulation index close to ∼1.5. However, at a nearly constant pressure of ∼0.8 atm, by the variation of operating temperature from 27^oC to 350^oC, modulation index is changed by 10%. Therefore, depending on the operating condition apodized amplitude can be maximized by the manipulating of the modulation index through changing the amplitude of modulation current.

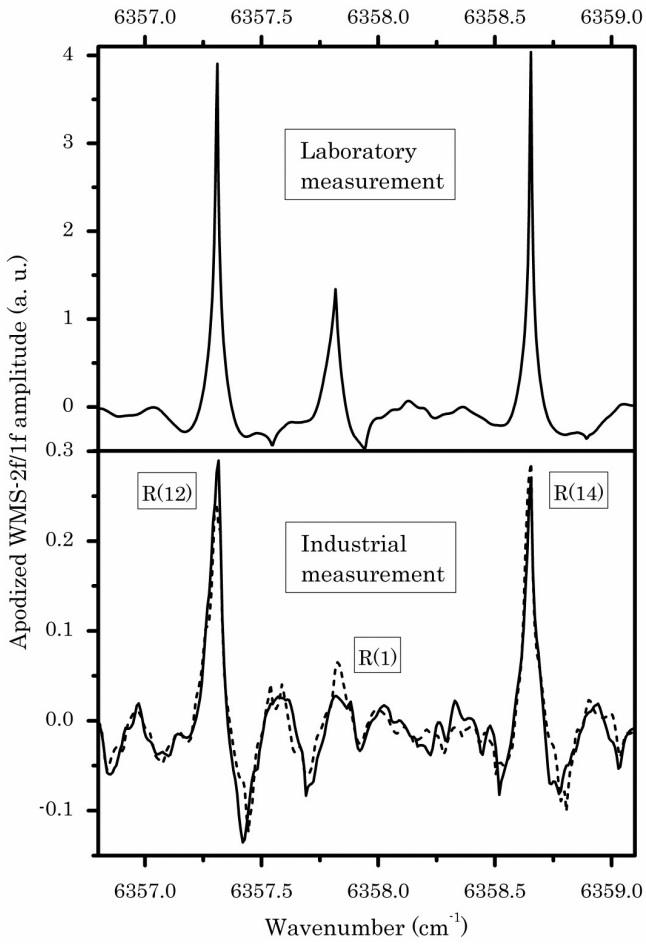

Figure 10. The On-line and in situ trace of targeted CO and CO_2 absorption lines in the recuperator channel of the selected stack at SMPP using the described apodized sensor system. The smoke was released at atmospheric pressure and temperature of $\sim 350^{o}$C. Modulation frequency and index were set to 3 kHz and 1.5, respectively. The scaling k factor and scanning period are 5 and 10 seconds, respectively. The reference measurement that performed in the laboratory is given for comparison. In the industrial measurement, solid and dashed lines are associated with two consecutive monitoring accomplished by one hour difference in one day.

3. Calibration-free apodized WMS-2f/1f gas sensor: Laboratory test

A reference measurement is performed based on the following experimental apparatus illustrated in Fig. 4 that was arranged in the laboratory to characterize the performance of the introduced gas sensor and to assign its capability in the outdoor application.

A light source with 5 mW output power was provided using a 1.57 μm DFB laser (Laser components GmbH.) that have a slope efficiency and tuning rate of 0.1 nm/K and 3.5 GHz/mA, respectively. The benefit of using such high performance laser source is the simultaneous trace detection of R(1) CO and R(12) and R(14) CO_2 overtone absorption lines in one period scanning of the laser current using a flexible ramp voltage. In order to establish the wavelength modulation a required sinusoidal wave with a flexible amplitude and index was generated using the designed electronics. The DFB output beam was delivered toward a 3-m-long glass tube using a 5-m-long single mode optical silica fiber (Tramco, 0652D). To avoid undesirable interferometric effects and not to confuse with the absorption trace the side windows of the glass cell were slightly inclined. The second 5-m-long multimode optical fiber (Thorlabs, M29L05) with a large diameter core of $\sim$600 μm was used at the opposite end of the cell to collect the transmitted light for the whole detection system including a high speed detector and a commercial data acquisition (DAQ, NI 6036E) card. The utilized detector was an InGaAs photodiode (Thorlabs, FGA20) that covered a relatively wide spectral range of 1400 nm from 1200 nm to 2600 with a high response time of 23 ns. Very flexible modulation frequency and index were provided by programming the PID code in the LabVIEW environment. Eventually, the active and precise control of the electronics and circuits was performed by the ultilized DAQ card. The advantage of the above system is the possibility of a relatively high sampling rate of $\sim$200 kS/s during the modulation of DFB wavelength. The digitized signal was demodulated using a lock-in amplifier to make X_{1f} and X_{2f} harmonic signals and to construct the final WMS-2f/1f output. A mixture of 68% CO and 32% CO_2 gases was respectively provided to obtain a total pressure of $\sim 690 \pm 0.1$ mbar inside the cell. The apodized WMS-2f/1f signal was produced using simultaneous modulation and scanning of the DFG laser over the absorption spectrum of R(1) CO and R(12) and R(14) CO_2 overtone lines. This was performed by a 32 mA ramp current and a 3 kHz modulation frequency. In Fig. 5 simultaneous detection of the targeted gases is illustrated.

Apparently, the performance of apodized WMS-2f/1f method is demonstrated in the trace of neighboring absorption features of the CO and R(12) CO_2 which are spaced by $\sim$0.5 cm^{-1}. Based on the obtained results, the peak height of the apodized WMS-2f/1f traces can be assumed as a criterion to obtain a reference curve for concentration calibration which we require for quantitative measurement at SMPP area. Fig. 6 shows the provided graph for determination of the percentage of CO and CO_2 molecules in the combustion smoke at the operating conditions similar to SMPP.

As it can be seen the apodized peak height shows a nearly linear variation with the CO and CO_2 concentrations with the slops of $\sim$0.015 and $\sim$0.028, respectively. Before, setting the sensor for outdoor application and in order to verify the performance of the demonstrated gas sensor the circumstance of SMPP area is simulated in the laboratory for making a confidential measurement on the emission of coal products. The coal combustion is one of the major resources of atmospheric pollutant which contains of a collective of toxic compounds. In a perfect combustion, coal burning yield CO_2 and water vapor. However, the presence of CO in the flue gas represents

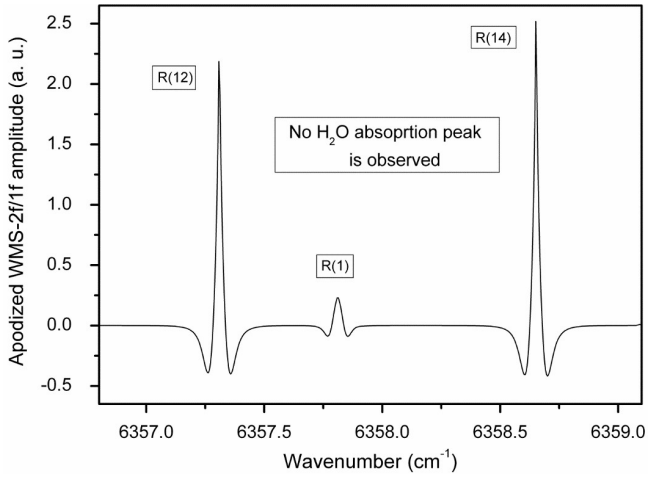

Figure 11. Simulated trace of R(1) CO, R(12) and R(14) CO_2 lines as well as the specified H_2O line for real situation within the spectral range of interest. The CO and CO_2 concentrations are assumed ∼1% and ∼9.5%, respectively, while for H_2O it is taken ∼2% according to the information given by SMPP daily report. The required parameters for simulation are the same as those used in Fig. 9.

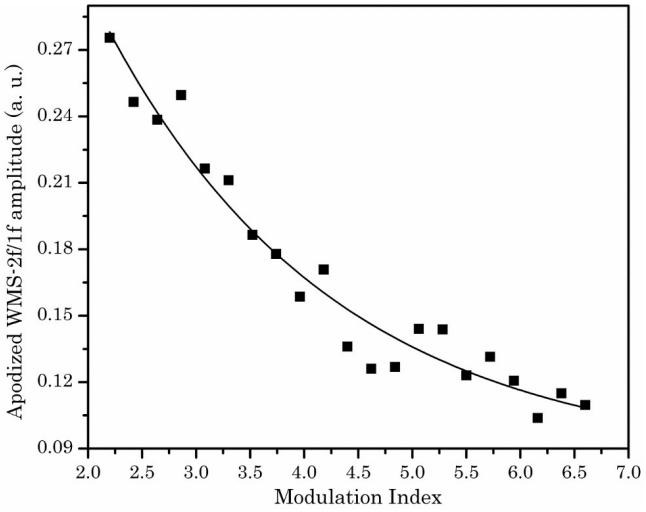

Figure 12. The effect of the modulation index on the strength of apodized trace measured for R(12) CO_2 line at SMPP area while the modulation frequency and scaling k factor have been fixed at 3 kHz and 5, respectively.

a state of incomplete combustion, which occurs mostly in the absence of sufficient air. However, the method of coal combustion also affects the emission products. Indeed, the formation of CO and CO_2 and their relative concentrations in the smoke of a typical coal combustion is dependent on the combustion temperature and the excess air. The analytical results shows that as the level of excess air is changed from 60 to 80%, the concentration of CO and CO_2 varies from 5 to 11% and from 3 to 8%, respectively [23].

The measurement is accomplished by collecting the realeasing smoke from the burning coal in a chamber and then flowed toward the fabricated 3-m-long glass tube. The mainstream of the coal smoke was then injected into the cell with a flow rate of ∼0.5 lit/min at atmospheric pressure. Simultaneously, the modulated DFB laser beam is scanned over the CO and CO_2 absorption lines to establish the apodized WMS-2f/1f signal. The results of this measurement are illustrated in Fig. 7.

As it can be seen, the trace of R(1) CO and R(12) and R(14) CO_2 lines have been sensitively resolved in the extracted smoke. From the results, concentrations of CO and CO_2 gases are estimated to be about 4% and 7%, respectively, which indicate very comparable with the reported results given in Ref. [24]. The sensitivity of this measurement is evaluated using a defined formula given as [24]

$$Sensitivity = \frac{A_{min}}{L\sqrt{\Delta f}} \tag{9}$$

where A_{min} is the minimum detectable absorption, L is the absorption path length and Δf is the effective detection bandwidth. Accordingly, the A_{min} can be obtained through [25]

$$A_{min} = \frac{\Delta V}{V} \tag{10}$$

where ΔV is the accuracy of measuring the output voltage passing by the detector and recorded by lock-in amplifier and V is the maximum of the output voltage receiving by DAQ card. By substituting the measured values of ΔV =1 kvolt and V =0.4 mvolt into Eq. (10) a minimum detectable senstitivity of $\sim 3.9\times10^{-4}$ is obtained. This led to a detection sensitivity of $\sim 1.3\times10^{-8}$ cm^{-1} $Hz^{-1/2}$ within ∼10 kHz of detection bandwidth of detection system. This feature expects that the apodized WMS-2f/1f spectrometer can be considered as a significant candidate for the fabrication of an in situ and on-line sensor for the monitoring of targeted gases in the industrial areas.

4. Calibration-free apodized WMS-2f/1f gas sensor: field measurement

In order to further examine the performance of the characterized apodized sensor an industrial and harsh area is used in the Isfahan suburb. The SMPP is located in the north part of the city and produces ∼1600 MW power electricity for industrial and public purpose. It utilizes a combined cycle of natural gas-fired furnaces which is known as huge producer of atmospheric pollution and greenhouse gases. The combustion products are delivered toward the environment by eight units each contains of two stacks with the emission capacity of 1000 m^3 per hour. The emitted products are released at a relatively high temperature range from ∼800 to ∼350^{o}C. Clearly, the emission of toxic and pollutant species can be minimized by quality control of the combustion through in situ and on-line monitoring of fuel gas during the combustion. To perform the

measurement, the experimental setup shown in Fig. 4, was miniaturized and embedded in an aluminum box ($30\times15\times15$ cm^3) to make the apodized sensor compact and portable. This was accomplished by replacing the bulky electronic devices to printed circuit boards in order to reduce the size of the spectrometer. This enabled to fully control the whole system by a DAQ card slot input devised on a programmed desktop computer. Fig. 8 shows the miniaturized experimental setup. As can be seen the output beam of the DFB laser is delivered toward a fabricated probe and the absorbed light is received by the detector at the same side using the two optical fibers that previously employed. The probe was fabricated from a 2-m-long stainless steel cylindrical tube for working at high operating temperature of $\sim350^oC$ to produce minimum thermal expansion and for protection against corrosion and stain when it is located inside the case stack which was provided by SMPP as a measurement pilot. As shown in Fig. 9, the sensor head was consisted of three reflecting 45^o prisms (BAK4, Schott Co.) embedded on the end sides of the probe. This configuration enabled DFB laser beam travelling four times between the designated prisms, establishing an effective optical path length of $\sim$8 meters. The setup is then aligned using two adjustable fiber-coupled collimators screwed on the probe such that the maximum intensity approaches the detector. To provide a required path for the DFB laser beam to be freely experienced by the fuel smoke, pairs of holes were made along the lateral surface of the tube on the opposite sides and sealed by very fine mesh grid to protect the internal optics against dust and soot particles. By this we further assured that the pressure inside and outside the tube are the equal.

Such described multipass and sealed probe was installed and located inside the recuperator channel of the stack. In order to cope with the environmental vibrations the collimation lenses were slightly defocused to decrease the sensitivity of alignment. The measurement was started by applying the referenced data were previously used in the scanning of the DFB laser over the targeted CO and CO_2 absorption lines. In Fig. 10 the results of this in situ and on-line measurement are indicated.

Clearly, as it is confirmed by the plot, the fabricated apodized WMS-2f/1f has shown good spectroscopic characteristics in the monitoring of selected gases inside the atmosphere of the channel. From the results, the CO and CO_2 concentrations are also measured as less than $\sim$1% and $\sim$9.5%, respectively, which are in agreement with the SMPP daily report which are providing based on the application of commercial gas sensors. Despite the presence of such relatively high CO concentration inside the channel, the R(1) CO line could not be significantly detected in the trace and discriminated from the background noise. This was because of the weak line strength of 8.25×10^{-24} cm^{-1}/(molecule cm^{-2}) for R(1) CO line around 1.57 μm.

Based on Eq. (9) and (10) an enhanced detection sensitivity of 4.8×10^{-9} cm^{-1} $Hz^{-1/2}$ is measured for 8-m-long absorption length and 10 kHz detection bandwidth. Indeed, the possible interference with water absorption lines is also investigated in this work. Referred to Hitran 2019 database, in the scanning range of the DFB laser the strongest H_2O line is centered at 6357.881 cm^{-1} and has a linestrength of 3.42×10^{-26} cm^{-1}/(molecule cm^{-2}) which is less than that of R(1), R(12) and R(14) lines by a factor of about three hundred. Taking into account both thermal and pressure broadenings we obtain a Doppler broadening of $\Delta\nu_D$ =0.027 cm^{-1} at 350^oC and pressure broadening of $\Delta\nu_L$ =0.0734 cm^{-1} at atmospheric pressure for the marked H_2O line, corresponding to a Voigt linewidth of $\Delta\nu_V$ =0.082 cm^{-1}. In Fig. 11 the abrosbance of the targeted lines of CO, CO_2 and H_2O lines is simulated within the spectral range of interest.

As it can be seen, even though the concentration of the water vapour is significant inside the channel, due to weak linestrength of the marked H_2O line no trace is obtained from the simulation and, therefore, the spectroscopic interference with the water line is not expected, confirming the experimental results depicted in Fig. 10.

The effect of modulation index on the strength of apodized WMS-2f/1f trace obtained in SMPP pilot is also investigated in Fig. 12.

As can be seen from the above plot, by increasing of the modulation index beyound two, the amplitude of apodized WMS-2f/1f signal is reduced. This can be connected to the results obtained through Fig. 3 where the maximum of modulation index was peaked around unity.

5. Conclusion

In this study, the performance of a gas sensor based on apodized WMS-2f/1f spectroscopy is investigated through simultaneous trace monitoring of the R(1) CO and R(12) and R(14) CO_2 absorption lines. This is performed using a tunable DFB laser operating around 1.57 μm. The study is supported by the theory and numerical simulation of the lineshapes of target molecules. A qualitative comparison is presented between the common and apodized WMS-2f/1f techniques to explain the drawbacks faced by the common approach mostly occurring beyond the optically thin limit which is undesirable for field applications. A quantitative investigation is also performed to provide a reference plot for percentage measurement of CO and CO2 concentrations under harsh industrial conditions. Theoretical results have been verified by the experiment in the laboratory scale using the output beam of a modulated DFB laser scanned over the selected lines which was directed toward a 3-m-long glass tube absorption cell containing 68% and 32% of pure CO and CO_2 gases, respectively. A quasi-industrial circumstance is simulated in the laboratory using the combustion of coal to examine the merits of the fabricated apodized WMS-2f/1f gas sensor. The appreciable characteristics of this measurement are indicated by the detection sensitivity measurement of 1.3×10^{-8} cm^{-1} $Hz^{-1/2}$. The utilized experimental set up is then miniaturized and brought into a box by the engineering of the bulky electronic devices and replacing them by predesigned circuit boards commanded

by the LabView instrumental control. Such described portable device is then equipped by a probe which was fabricated from a 2-m-long stainless steel tube, providing an effective absorption path length of $\sim$8 m using three reflecting 45^o prisms embedded on the ends sides of the cylindrical tube to make quadruple round-trip for the transmitted laser beam. The fabricated probe is then placed into the recuperator channel of the pilot stack at SMMP industry for on-line and in situ monitoring of the selected absorption lines at atmospheric pressure inside the released smoke. The excellent performance of the apodized sensor is shown by the measured detection sensitivity of $\sim 4.8\times10^{-9}$ cm^{-1} Hz$^{-1/2}$ which indicates a considerable growth compared with the results obtained in the laboratory scale. This led to the CO and CO_2 concentration measurement of less than $\sim$1% and $\sim$9.5%, respectively, at 350^oC which is performed under a very real and harsh situation, showing close agreement with the reference data provided by SMPP's daily report.

Conflict of interest statement:
The authors declare that they have no conflict of interest.

References

[1] M. Lackner. *Reviews in Chemical Engineering*, **23**:65, 2007.

[2] F. K. Tittel, G. Wysocki, A. Kosterev, and Y. Bakhirkin. *Mid-Infrared Coherent Sources and Applications- Conference paper*, :467, 2008.

[3] S. Solga, M. Mudalel, L. Spacek, R. Lewicki, F. K. Tittel, C. Loccioni, A. Russo, A. Ragnoni, and T. Risby. *J. Breath research*, **8**:037103, 2014.

[4] M. Mohammadi Jozdani, A. Khorsandi, and S. Ghavami Sabouri. *Appl. Phys. B*, **118**:219, 2015.

[5] H. Li. *Photonic Sensors*, **6**:127, 2016.

[6] S. Koch, F. Jahnke, and W. Chow. *Semiconductor science and technology*, **10**:739, 1995.

[7] W. Zeller, L. Naehle, P. Fuchs, F. Gerschuetz, L. Hildebrandt, and J. Koeth. *Sensors*, **10**:2492, 2010.

[8] X. Liu, P. Stefanou, B. Wang, T. Woggon, T. Mappes, and U. Lemmer. *Optics express*, **21**:28941, 2013.

[9] H. Qi, Z. Song, S. Li, J. Guo, C. Wang, and G. D. Peng. *Optics express*, **21**:11309, 2013.

[10] M. Bagheri, G. Spiersa, M. Fradet, and S. Forouhar. *18th Coherent Laser Radar Conference*, **724**:456, 2016.

[11] D. M. Sonnenfroh and M. G. Allen. *Applied optics*, **36**:3298, 1997.

[12] T. Cai, G. Gao, W. Chen, G. Liu, and X. Gao. *Applied Spectroscopy*, **65**:108, 2011.

[13] H. B. Yu, W. Jin, H. L. Ho, K. C. Chan, C. C. Chan, M. S. Demokan, G. Stewart, B. Culshaw, and Y. B. Liao. *Applied Optics*, **40**:1011, 2001.

[14] Z. Li, W. Ma, X. Fu, W. Tan, G. Zhao, L. Dong, L. Zhang, W. Yin, and S. Jia. *Optics express*, **21**:17961, 2013.

[15] A. Maity, M. Pal, S. Maithani, G. Dutta Banik, and M. Pradhan. *Laser Physics Letters*, **15**, 2018.

[16] M. R. McCurdy, Y. A. Bakhirkin, G. Wysocki, R. Lewicki, and F. K. Tittel. *Journal of Breath Research*, **1**:014001, 2007.

[17] J. Wojtas, F.K. Tittel, T. Stacewicz, Z. Bielecki, R. Lewicki, J. Mikolajczyk, N. Nowakowski, D. Szabra, P. Stefanski, and J. Tarka. *Intl. Journal of Thermophysics*, **35**:2215, 2014.

[18] A. A. Kosterev, D. V. Serebryakova, A. L. Malinovsky, and I. V. Morozov. *Scientific Instruments*, **76**:043105, 2005.

[19] H. Li, G. B. Rieker, X. Liu, J. B. Jeffries, and R. K. Hanson. *Applied Optics*, **45**:1052, 2006.

[20] G. B. Rieker, J. B. Jeffries, and R. K. Hanson. *Appl. Opt.*, **48**:5546, 2009.

[21] C. Goldenstein, R. Spearrin, I. Schultz, J. Jeffries, and R. Hanson. *Measurement Science and Technology*, **25**:055101, 2014.

[22] S. Hosseinzadeh Salati and A. Khorsandi. *Applied Physics B*, **116**:521, 2014.

[23] J. C. Chen, A. S. Liu, and J. S. Huang. *J. of Hazard Mater.*, **142**:266, 2007.

[24] D. Heard. *Analytical techniques for Atmospheric measurement*. Blackwell publishing Ltd, 1th edition, 2006.

[25] Nikolai V. Techenko. *Optical Spectroscopy: Methods and Instrumentations*. Elsevier, 2006.